

DOI: 10.1002/cplu.201300299

Real-Time Monitoring of the Dephosphorylating Activity of Protein Tyrosine Phosphatases Using Microarrays with 3-Nitrophosphotyrosine Substrates

Jeroen van Ameijde,^[a, b] John Overvoorde,^[c] Stefan Knapp,^[d] Jeroen den Hertog,^[c, e]
Rob Ruijtenbeek,^[f] and Rob M. J. Liskamp^{*[a, g]}

Phosphatases and kinases regulate the crucial phosphorylation post-translational modification. In spite of their similarly important role in many diseases and therapeutic potential, phosphatases have received arguably less attention. One reason for this is a scarcity of high-throughput phosphatase assays. Herein, a new real-time, dynamic protein tyrosine phosphatase (PTP) substrate microarray assay measuring product formation is described. PTP substrates comprising a novel 3-nitrophosphotyrosine residue are immobilized in discrete spots. After reaction catalyzed by a PTP a 3-nitrotyrosine residue is formed that can be detected by specific, sequence-independent antibodies. The resulting microarray was successfully evaluated with a panel of recombinant PTPs and cell lysates, which afforded results comparable to data from other assays. Its parallel nature, convenience, and low sample requirements facilitate investigation of the therapeutically relevant PTP enzyme family.

Phosphatases and kinases regulate the crucial phosphorylation post-translational modification. In spite of their similarly important role in many diseases and therapeutic potential, phosphatases have received arguably less attention. One reason for this is a scarcity of high-throughput phosphatase assays. Herein, a new real-time, dynamic protein tyrosine phosphatase (PTP) substrate microarray assay measuring product formation is described. PTP substrates comprising a novel 3-nitrophosphotyrosine residue are immobilized in discrete spots. After reaction catalyzed by a PTP a 3-nitrotyrosine residue is formed that can be detected by specific, sequence-independent antibodies. The resulting microarray was successfully evaluated with a panel of recombinant PTPs and cell lysates, which afforded results comparable to data from other assays. Its parallel nature, convenience, and low sample requirements facilitate investigation of the therapeutically relevant PTP enzyme family.

Introduction

Phosphatases and kinases control the vital phosphorylation post-translational modification.^[1] Aberrant activity of these enzymes causes diseases, for example, cancer and diabetes, and they are valuable therapeutic targets.^[2] Arguably, up to now focus has been more on kinases than phosphatases, largely because high-throughput phosphatase assays remain scarce,^[3] examples include starting-material consumption-based microarrays,^[4] a recent high-throughput endpoint enzyme-linked im-

munosorbent assay (ELISA) setup,^[5] an endpoint assay in which the tyrosine produced is oxidized by tyrosinase and then detected,^[6] and a method involving a 3-fluoromethylphosphotyrosine moiety that can covalently bind a phosphatase.^[7] It should be noted that high-throughput screens of compound libraries against individual phosphatases have been reported (e.g., against diabetes target PTP1B and cancer target PTEN). However, these typically involved simple phosphate derivatives as substrate models instead of the more realistic phosphopeptidic substrates applied in the assay described here. In addition, the ability to study many potential substrates of protein tyrosine phosphatases in parallel is virtually nonexistent and ultimately essential for development of selective therapeutics.

Herein, we present a new dynamic, sensitive, high-throughput protein tyrosine phosphatase (PTP) substrate microarray assay based on the detection of product formation. It comprises substrates with a novel 3-nitrophosphotyrosine building block. Dephosphorylation by a PTP leaves a 3-nitrotyrosine residue that can be detected by selective, sequence-independent antibodies, which uniquely allows a real-time product-formation assay (Figure 1A). Since a non-proteinogenic amino acid is formed, it can only result from PTP activity. Recently, an alternative method for the detection without antibodies of 3-nitrotyrosine formed through chemical derivatization was described.^[8] Modeling studies based on existing crystal structures of PTPs with phosphopeptides as well as the studies on 3-fluoromethylphosphotyrosine residues^[7] demonstrate that the active sites in PTPs can accommodate relatively small modifications of phosphotyrosine substrates. This is illustrated, for example, by the model of SHP1^[9] with a 3-nitro-modified peptide derived from a SHP1 substrate (Figure 1B). PTPs are a highly relevant enzyme family, which includes tumor suppressors

[a] Dr. J. van Ameijde, Prof. Dr. R. M. J. Liskamp
Medicinal Chemistry and Chemical Biology
Utrecht University
Universiteitsweg 99, 3584 CG Utrecht (The Netherlands)
Fax: (+31)(0)30-253-6655
E-mail: r.m.j.liskamp@uu.nl
robert.liskamp@glasgow.ac.uk

[b] Dr. J. van Ameijde
Netherlands Proteomics Centre
Padualaan 8, 3584 CA Utrecht (The Netherlands)

[c] Dr. J. Overvoorde, Prof. Dr. J. den Hertog
Hubrecht Institute, KNAW and University Medical Centre
Uppsalalaan 8, 3508 AD Utrecht (The Netherlands)

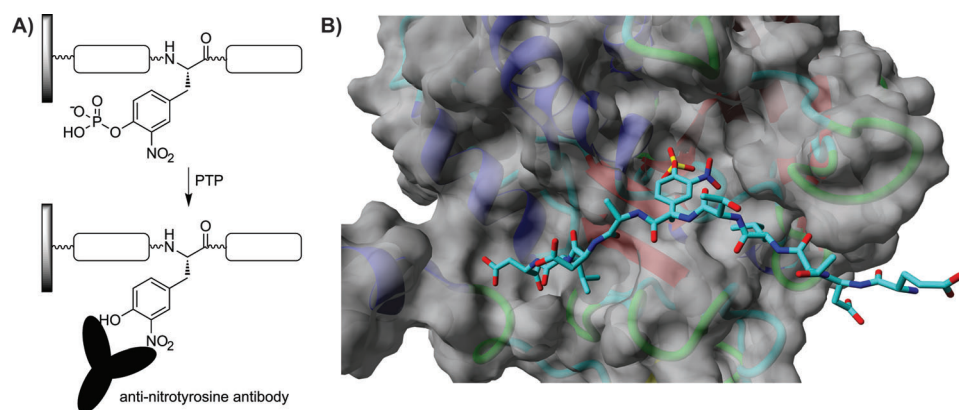
[d] Prof. Dr. S. Knapp
Structural Genomics Consortium, Oxford University
Roosevelt Drive, Headington, Oxford OX3 7DQ (U.K.)

[e] Prof. Dr. J. den Hertog
Institute of Biology, Leiden University
P.O. Box 9502, 2300 RA Leiden (The Netherlands)

[f] Dr. R. Ruijtenbeek
Pamgene International Ltd.
Wolvenhoek 10, 5200 BJ Den Bosch (The Netherlands)

[g] Prof. Dr. R. M. J. Liskamp
School of Chemistry, Joseph Black Building
Glasgow University
University Avenue, Glasgow G12 8QQ (U.K.)

 Supporting information for this article is available on the WWW under <http://dx.doi.org/10.1002/cplu.201300299>.

**Figure 1.**

A) 3-Nitrophosphotyrosine detection strategy. B) Model of a 3-nitrophosphotyrosine peptide in the active site of SHP1 based on PDB entry 1FPR.^[9]

DEP1 and GLEPP1,^[10] diabetes target PTP1B,^[11] and carcinoma-associated PTP γ .^[12]

To the best of our knowledge, no product-formation microarray assay exists for real-time, dynamic measurement of phosphatase activity. Advantages of this detection mode over consumption of the starting material include no competition for the substrate between the phosphatase and the detecting antibody, increased sensitivity, and avoidance of problems associated with detector-signal saturation. Indeed, experiments with a phosphotyrosine antibody that could measure starting-material consumption gave rise to significantly lower signals than those that will be presented here. Furthermore, such an assay requires that the antibody instantly binds the large amount of starting material present at the start of the assay. We have found in this and similar microarray assays that antibodies are often incapable of achieving rapid binding and the kinetic read-out obtained is actually a complicated combination of antibody binding and substrate consumption hampering data analysis. A product-formation assay for PTPs might involve antibodies against tyrosine; however, in our hands such antibodies failed to detect PTP products strongly and independently of sequence. Furthermore, such a detection strategy is clearly sensitive to additional tyrosines present in the substrate sequence.

Alternatively, detecting the inorganic phosphate formed^[13] is unsuitable for microarrays since the phosphate will diffuse away from the substrate spot and it is therefore impossible to monitor multiple substrates in parallel. Furthermore, such methods are clearly sensitive to the presence of bulk phosphate in a sample. Finally, except for the coupled assay developed by Webb,^[13c] only endpoints can be determined and dynamic measurements are impossible. The 3-fluoromethylphosphotyrosine strategy mentioned above^[7] is impractical for microarrays since all PTPs to be evaluated would have to be labeled, which is also impossible in lysates.

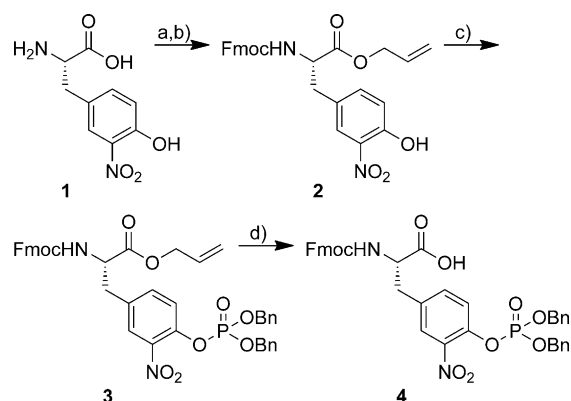
The assay presented here uniquely combines a parallel, high-throughput nature, dynamic real-time measurement of product formation without the potential problems outlined

above for measuring starting-material consumption, and compatibility with complex biological matrices. In addition, the underlying technology has already been successfully targeted for kinases, lectins, and nuclear hormone receptors,^[14] which opens up the intriguing prospect of studying different enzyme families with the same assay setup. Apart from an extensive validation of this new platform, several applications will be described: substrate profiling of PTPs, inhibitor evaluation as well as studies on cell lysates.

Results and Discussion

Preparation microarray

3-Nitrophosphotyrosine monomer **4** (Scheme 1) was prepared in three steps from 3-nitrotyrosine (**1**). First, *N*-(fluorenyl-9-methyloxycarbonyl) (Fmoc) and allyl protecting groups were



Scheme 1. Synthesis of phosphonitrotyrosine monomer **4**. a) 1. Fmoc-OSu (OSu = succinimide), diisopropylethylamine (DiPEA), dioxane/water 1:1 v/v. b) Allyl bromide, DiPEA, DMF, 0°C to RT (92% overall). c) *O,O*-Dibenzyl-*N*-diisopropylphosphoramidate, tetrazole, THF (73%). d) [Pd(PPh₃)₄], *N*-methylamine, THF (91%). Bn = benzyl, DMF = *N,N*-dimethylformamide, THF = tetrahydrofuran.

introduced, which resulted in near-quantitative formation of **2** that could be purified by crystallization. The phenolic hydroxyl group was then phosphorylated using phosphoramidate chemistry to yield fully protected **3**, after which the allyl group was removed in near-quantitative yield under Pd⁰ catalysis to afford monomer **4** in 61% overall yield on a 2.7 g scale. This monomer was incorporated into 9 peptides derived from endogenous PTP substrates^[7,15] with 4 to 5 flanking residues on both sides and an *N*-terminal cysteine–glycine dipeptide for

Table 1. Substrate sequences.			
Substrate ^[a]	Uniprot ^[b]	Sequence ^[c]	Description
CADH2 (780–789)	P19022	CG-EEDQD(NO ₂ -pY)DLSQ	cadherin-2 (neural cadherin)
PDPK1 (4–13)	O15530	CG-TTSQL(NO ₂ -pY)DAVP	phosphoinositide-dependent protein kinase 1
ZAP70 (287–296)	P43403	CG-LNSDG(NO ₂ -pY)TPEP	70 kDa zeta-associated protein
PGFRB (746–755)	P09619	CG-DESVD(NO ₂ -pY)VPBL	B-type platelet-derived growth factor receptor
GHR (591–600)	P10912	CG-PVPD(NO ₂ -pY)TSHI	growth hormone receptor
CSK (179–188)	P41240	CG-AQDEF(NO ₂ -pY)RSGW	c-Src kinase
SIGLEC2 (817–826)	P20273	CG-DEGIH(NO ₂ -pY)SELI	B-cell receptor CD22
STAT3 (701–709)	P40763	CG-SAAP(NO ₂ -pY)LKTK	signal transducer and activator of transcription 3
JAK2 (1002–1011)	O60674	CG-PQDKE(NO ₂ -pY)YKVK	Janus kinase 2

[a] Numbers in parentheses indicate the location of the sequence in the parent protein. [b] Entries taken from the Universal Protein Resource. [c] One-letter abbreviation B denotes a norleucine residue and NO₂-pY refers to the new 3-nitrotyrosine residue.

surface attachment through maleimide chemistry (Table 1). The selected substrates all have therapeutic relevance, for example, SIGLEC2 for autoimmune diseases^[16] and ZAP70 in leukemia.^[17]

Although we initially had some concerns regarding the stability of the peptides because of the increased leaving-group character imparted by the nitro substituent, no stability issues were observed during synthesis and purification by reversed-phase HPLC. Furthermore, the peptides could be stored in a dry form for at least 6 months at -20°C without any degradation as was judged by HPLC. Some degradation was observed after prolonged storage in buffer; however, all peptides remained intact on assay timescales (up to several hours) in typical assay buffers.

All substrate peptides were printed onto a PamChip microarray^[18] in a concentration series (125–1000 μM , referred to as ‘spot concentration’), as well as a non-phosphorylated 3-nitrotyrosine peptide derived from Stat3 as a positive control. The material used consists of a porous surface that improves the extent of immobilization and thus sensitivity. Moreover, the analyte can be repeatedly pumped through the array, thereby improving mixing and allowing imaging while the droplet with bulk background fluorescence is below the surface. This enables real-time, dynamic monitoring and therefore kinetic analysis. Although several combinations of anti-nitrotyrosine antibodies (HM11, 39B6),^[19] secondary antibodies (fluorescein isothiocyanate (FITC)-labeled or Cy3-labeled, goat anti-mouse, bovine anti-mouse), and buffers (phosphate, tris(hydroxymethyl)aminomethane (Tris), 4-(2-hydroxyethyl)-1-piperazineethanesulfonic acid

(HEPES)) were applied successfully, in all further experiments HM11, FITC-labeled goat anti-mouse, and phosphate buffer will be used since this combination resulted in optimal signal-to-noise ratios. HM11 detected all substrates irrespective of flanking residues as determined by treating the array with non-selective alkaline phosphatase. Monoclonal 3-nitrotyrosine antibody 1A6^[20] was evaluated as well since its FITC conjugate is commercially available, which eliminates the need for a secondary antibody. However, this particular clone failed to detect all substrate sequences.

Enzymological validation

Figure 2 shows data for PTP DEP1 (detailed data for all experiments with recombinant PTPs, PTP inhibitors, and cell lysates

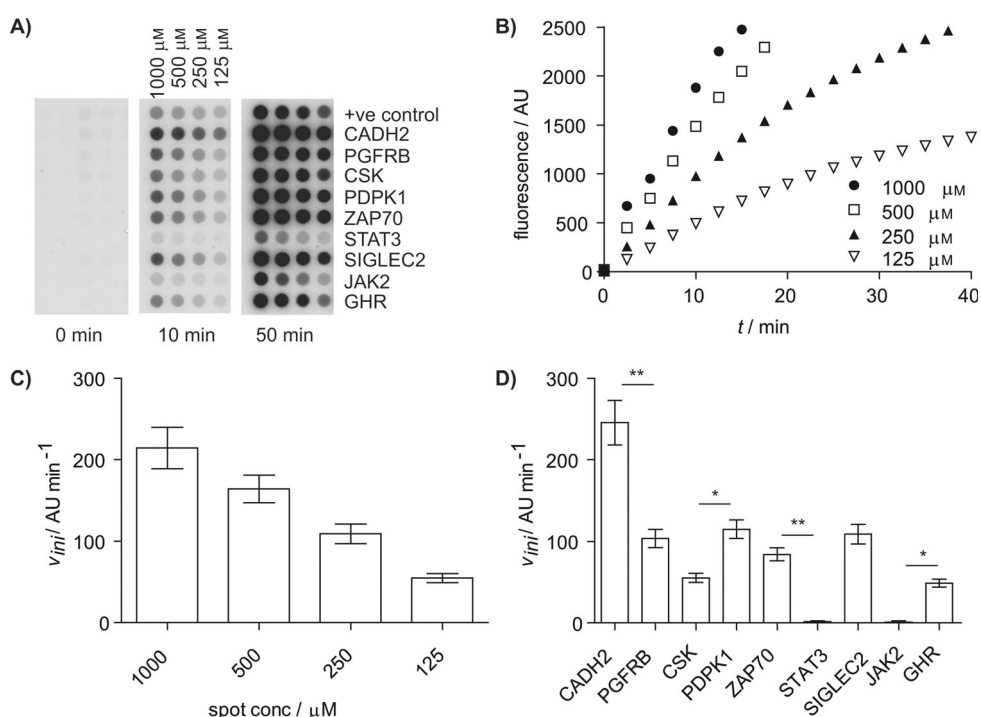


Figure 2. Sample data for DEP1. All data is averaged ($n=6$). Error bars correspond to the standard error of the mean (s.e.m.). A) Fluorescence microscopy images at different time points. B) Progress curves. C) v_{ini} for the SIGLEC2 at different spot concentrations. D) Selectivity profile at 250 μM (* $P < 0.05$; ** $P < 0.01$).

described in this study are included in the Supporting Information), which is of interest from a cancer drug development perspective.^[10a-b] The activities of all recombinant enzymes added were standardized at 0.5 mU against *p*-nitrophenylphosphate (pPNP) per array. An untreated array was used as a negative control in all assays. The fluorescence images (Figure 2A) and the resulting time courses (Figure 2B) showed signal increase over time and thus dephosphorylation by DEP1. Initial velocities (v_{ini}) calculated from the curves (Figure 2C) demonstrated a dependence on spot concentration and therefore on substrate concentration. Performing this calculation for all substrates gave an activity profile for DEP1 against all 9 substrates on the array in a single run (Figure 2D). Statistically significant differences were observed, for example, JAK2 and STAT3 were poor substrates in this case.

Next, the array was validated with PTP GLEPP1, and studied as a tumor suppressor in the context of leukemia and lung cancer^[10c-d] (Figure 3). Plots of v_{ini} against spot concentration (Figure 3A) conformed to Michaelis–Menten kinetics, and 0.05 mU of enzyme was sufficient for strong fluorescent signals. Typical PTP concentrations used here, determined with the bicinchoninic acid (BCA) protein assay, were several orders of magnitude lower than the spot concentration as required for Michaelis–Menten behavior. Calculated Michaelis constant (K_m) values (Figure 3B) were comparable to those reported for PTPs with peptidic substrates.^[21] It should be noted that in determining these K_m values, spot concentration was used as a measure for substrate concentration, which therefore refers to immobilized compounds. Still, these ' $K_{m,het}$ ' values were in the same range as typical conventional K_m values and may therefore serve as a good indicator. In any case, for comparison of different PTPs, for example, for the relative potencies of two

inhibitors or lysates of cells grown under different conditions, only relative data is required irrespective of precise substrate concentrations.

To further determine the possible influence of both immobilization of the peptidic substrate and presence of a nitro substituent on the tyrosine residue, a comparison was made with the homogeneous EnzChek phosphate assay.^[13c] To this end, peptide substrates derived from PTP substrates STAT3, ZAP70, and LCK containing an unmodified phosphotyrosine residue and the corresponding 3-nitrophosphotyrosine-containing peptides were evaluated in this assay and compared to the microarray data with four PTPs. Either inorganic phosphate solutions or a concentration series of non-phosphorylated 3-nitrotyrosine-containing STAT3 spotted onto the microarray were used for calibration. The enzyme concentration was estimated with the BCA protein assay. The resulting kinetic parameters (K_m , k_{cat} , and k_{cat}/K_m) are summarized in Table 2. These data unambiguously showed that consistent results were obtained in all cases without significant influence of either immobilization or the 3-nitro substituent. This was especially evident from k_{cat}/K_m , which is a measure of substrate specificity. Interestingly, in this microarray setup all kinetic parameters were obtained in one experiment underlining its power. Although these specific kinetic parameters have not been reported in the literature, PTPs with nitrophenyl phosphate substrates as well as other PTPs with peptidic substrates generally give similar values.^[4d,22,23] Furthermore, a k_{cat} of $(44 \pm 3) s^{-1}$ was determined for PTP1B with the STAT3 substrate with the microarray, which is comparable to literature data for PTP1B with *para*-nitrophenyl phosphate $((23.8 \pm 0.7) s^{-1})$.^[22b] The microarray gave a comparable value of $(26 \pm 1) s^{-1}$ with the STAT3 peptide. Taken together, these experiments clearly demonstrated that immobili-

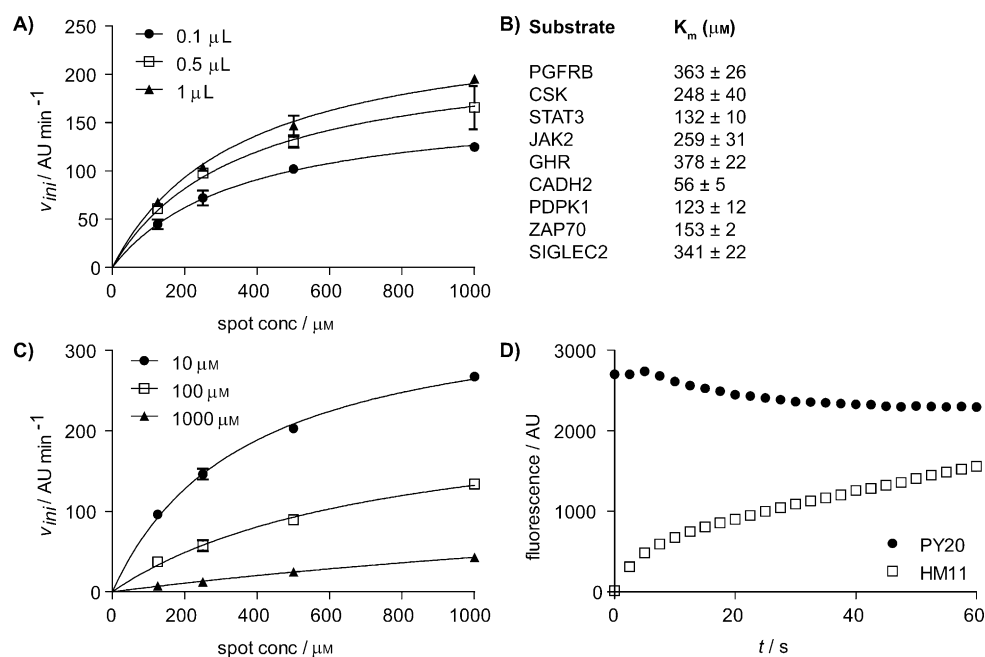


Figure 3. Validation of the PTP microarray. A) Nonlinear global fit of GLEPP1 with the JAK2 substrate peptide (averages with $n=4$; $1 \mu L$ corresponds to 0.5 mU; error bars correspond to the s.e.m.). B) K_m values for GLEPP1 with different substrates ($n=4$). C) Nonlinear global fit of GLEPP1 with the JAK2 peptide and sodium vanadate added ($n=4$). D) Detecting product formation versus starting material consumption for PTP1B with the STAT3 substrate ($n=6$).

Table 2. Comparison of kinetic constants.

Substrate/enzyme ^[a]		K_m [μM]	k_{cat} [s^{-1}]	k_{cat}/K_m [$10^4 \text{ M}^{-1} \text{ s}^{-1}$]
STAT3/GLEPP1	H	206 ± 33	1.1 ± 0.1	0.54 ± 0.08
	N	133 ± 21	0.92 ± 0.07	0.69 ± 0.12
	NI	132 ± 10	0.68 ± 0.03	0.51 ± 0.07
LCK/SHP2 ^[b]	H	672 ± 216	17 ± 4	2.6 ± 0.6
	N	460 ± 77	27 ± 3	5.9 ± 0.8
ZAP70/PTP γ	H	167 ± 67	8.7 ± 0.6	5.2 ± 0.7
	N	195 ± 32	11 ± 1	5.8 ± 0.9
	NI	126 ± 8	6.8 ± 0.3	5.4 ± 0.6
LCK/PTP κ ^[b]	H	169 ± 25	14 ± 1	9 ± 1
	N	349 ± 88	20 ± 3	5.1 ± 0.8

[a] H denotes a substrate containing a phosphotyrosine moiety, N denotes the corresponding 3-nitrophosphotyrosine substrate peptide. NI denotes immobilized 3-nitrophosphotyrosine peptide. [b] LCK is a peptide derived from lymphocyte-cell-specific protein-tyrosine kinase p56 (P06239), residues 389–399.

zation and the 3-nitro moiety did not influence enzymological results, that spot concentrations could be used as a measure for substrate concentration, and therefore that this new multiplex setup generated consistent enzymological data.

Inhibitor evaluation

Adding non-specific phosphatase inhibitor sodium vanadate confirmed that the activity observed was indeed PTP-mediated (Figure 3C). The inhibition constant (K_i) of 100–200 μM depending on substrate is reasonable in a dithiothreitol (DTT)-containing buffer.^[24] Additionally, known inhibitor NSC87877^[25] was tested with SHP2 giving a low micromolar K_i value, which agrees with reported data.

Comparison of detection modes

As stated in the Introduction, one of the attractive properties of this assay is the product-formation detection mode. Since we found that phosphotyrosine antibody PY20 also recognizes the 3-nitrophosphotyrosine residue introduced here, both possible detection modes could be compared directly. Figure 3D shows time courses for PTP1B with the STAT3 substrate on separate arrays with either PY20 (substrate consumption) or HM11 (product formation) as the detecting antibody. Similar rate constants were calculated (6.9×10^{-4} and $5.2 \times 10^{-4} \text{ s}^{-1}$, respectively). However, the PY20 experiments clearly showed problems at the start of kinetic runs because of signal saturation and the inability of the antibody to instantly bind all substrate molecules available. Because of this, it was difficult even to measure curves that could be used for data analysis. Furthermore, the PY20 curve had a threefold lower dynamic range. Thus, a product-formation assay as is described here is preferred over an assay that measures substrate consumption.

Profiling PTP panel

The heatmap in Figure 4 shows profiles for 17 PTPs at 250 μM spot concentration. At this spot concentration and enzyme load (0.5 mU) all combinations of substrate and PTP could be studied under equal conditions. However, for profiling certain individual PTPs a lower enzyme load would have been desirable, since lowering the signals leads to an increased dynamic range and therefore larger discrimination between substrate peptides. The Z' -factor is a statistical gauge for which a value above 0.5 means an assay is suitable for high-throughput purposes.^[26] Using the non-phosphorylated 3-nitrotyrosine-containing STAT3 peptide as the positive control and experiments in the absence of PTPs as the negative control, an average Z' -factor of 0.81 was determined. Two inactive PTP mutants were included as controls, C433S-C723S PTP α and A462T SHP2,^[27]

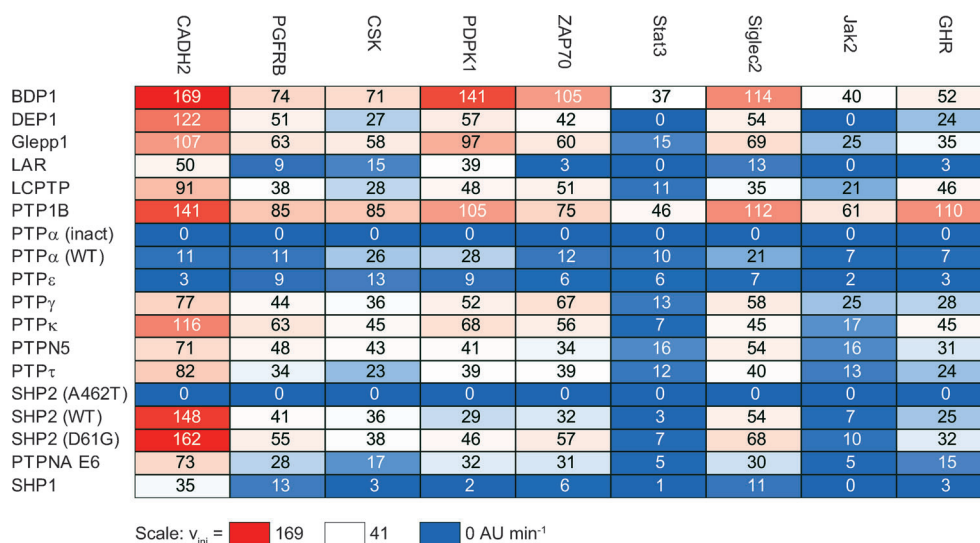


Figure 4. Heatmap PTP profiling experiments. The numbers are averages of the v_{ini} corrected for an untreated array ($n = 6$). Coloring proportional to v_{ini} with dark red highest and dark blue lowest.

and indeed gave no signal in contrast to the corresponding wild-type (WT) PTPs. In contrast, constitutively activated mutant D61G SHP2^[27] displayed significantly increased activity ($P < 0.01$) relative to WT SHP2. This mutant is the cause of Noonan's Syndrome, a genetic disorder, which, amongst others, leads to severe growth defects and congenital heart disease. The possibility to observe differences in activity with the new microarray assay may aid in diagnostics on aberrant SHP2 activity.

In general, profiling data followed trends similar to literature data,^[7,15] for example, PTP1B, GLEPP1, and DEP1 are promiscuous and efficient, in contrast to PTP α and PTP ϵ , and the CADH2 phosphopeptide is a good substrate for many PTPs. There are, however, certain differences such as the strong activity of BDP1, although even in this case the selectivity profile was comparable.^[15] Although substrate peptides of similar lengths have been applied in the literature, differences in PTP affinity and selectivity observed may be remedied by immobilizing longer substrate peptides or a longer spacer between peptide and surface, which is in fact possible in the setup presented here. Furthermore, as stated above, the uniform enzyme load applied in the profiling experiments may have to be lowered when studying certain PTPs to obtain optimal substrate discrimination. Additionally, expanding the substrate set may lead to even more discriminating profiles. As an example of this, the Supporting Information contains initial results for experiments using an expanded PTP microarray with 27 substrates. Where this extended array overlapped with the substrate described in this study, a similar profile was obtained for PTP1B. Furthermore, the inactive A462T SHP2 mutant again gave no appreciable dephosphorylation. In addition, a profile obtained for a WT HEK293 lysate overlapped well with the data presented below for the smaller array.

Most importantly, these profiles cover many substrate–PTP combinations that have not been studied before and may be valuable for elucidating signaling networks involving PTPs. For example, LAR preferentially recognizes the CADH2 and PDPK1 substrate peptides. Although the association with cadherins is known,^[28] this link with PDPK1 has not been described before although PDPK1 activity is regulated by a PTP, which is of interest given the role of PDPK1 in cancer.^[29]

Cell lysate experiments

Finally, PTP activity was monitored in WT HEK293 cell lysates (Figure 5A). Even 0.5 μg of total protein was sufficient for reproducible data. Then, HEK293 cells transiently transfected with WT PTP1B or inactive C215S PTP1B^[30] were applied (Figure 5B). WT PTP1B cells gave stronger dephosphorylation of all peptides except JAK2 and STAT3 compared to non-transfected control, consistent with the PTP1B profile in Figure 4. The C215S cells gave significantly lower signals compared to WT PTP1B cells for all substrates except JAK2 and STAT3 as expected. Treatment of the C215S lysate with 250 μM sodium vanadate (Figure 5C, column C215S-VO4) led to significant further reduction in activity, which demonstrates that residual activity in this lysate was due to other PTPs. The C215S lysate spiked

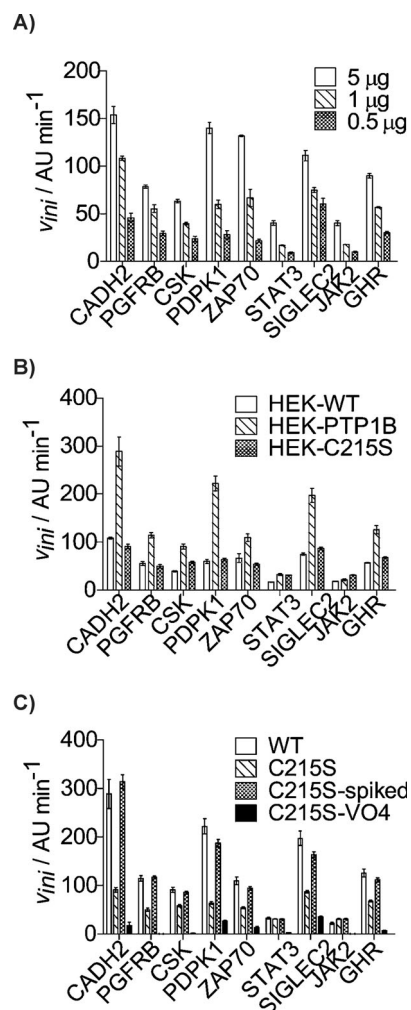


Figure 5. Cell lysate experiments. A) Concentration series WT HEK293 lysate (averages with $n = 6$; amounts correspond to total protein content; error bars correspond to the s.e.m.). B) Comparison of PTP WT HEK293 lysate and HEK293 lysate transfected with active PTP1B and inactive C215S PTP1B ($n = 6$). C) v_{ini} values obtained for HEK293 lysates treated with vanadate or spiked with recombinant PTP1B ($n = 12$).

with 1 mU PTP1B (Figure 5C, column C215S-spiked) showed recovered activity for all substrates except JAK2 and STAT3 as expected. PTP1B is arguably the most studied PTP since it is a promising diabetes type 2 drug target,^[11] although establishing and obtaining selectivity of potential inhibitory drugs has been challenging. Therefore, the ability to study PTP1B activity in lysates in a parallel fashion offered by this new microarray assay is extremely valuable.

Conclusion

In conclusion, the various biological experiments presented here demonstrate the general applicability of the new dynamic product-formation PTP substrate microarray. Consistent data was obtained with 17 PTPs irrespective of the 3-nitro modification at low enzyme loads. It is tremendously encouraging that even a relatively small substrate set yielded useful specificity data and that complex biological matrices can be studied as

well. Clearly, expanding the substrate set will lead to even more discriminating profiles. The parallel nature of the new microarray is a distinct advantage over nonmicroarray formats, allowing rapid profiling of substrate specificity, inhibitor potency, and enzymological parameters. Further attractive properties of this particular microarray are its dynamic nature, product-formation detection mode, and compatibility of the underlying technology with other enzyme families^[14] offering the enticing prospect of studying multiple enzyme classes with one experimental setup.

Experimental Section

General

Synthetic procedures, NMR spectra, MS spectra, and HPLC chromatograms are included in the Supporting Information.

Microarray preparation

All substrate peptides were spotted onto PamChip FAEC chips (PamGene International Ltd.), which are themselves based on Anopore aluminum oxide membranes (Whatman) functionalized with a spacer terminating in a maleimide group. A Scienion SciFlexArrayer S11 spotter was used to spot each premade (300 μL), centrifuged (3200 rpm, 5 min) solution of the individual substrates in Milli Q (MQ) water in the presence of 1 mM *tris*(2-carboxyethyl)-phosphine (TCEP). The resulting full arrays were dried for 5 min at 20 °C. After spotting, the remaining maleimide functionalities were inactivated by washing consecutively with 10 mM thiol-polyethylene glycol (PEG) (Mercachem) in phosphate buffer saline (PBS) solution, PBS, and MQ water. The final arrays were dried for 10 min at 20 °C. A quality control was carried out in which a full array was stained with SYPRO Ruby (Bio-Rad Laboratories) to quantify the peptide immobilization for all spots.

Expression of recombinant PTPs and activity assays

Recombinant PTP proteins were produced as glutathione-S-transferase (GST) fusion proteins in bacteria and purified using standard protocols. pGEX-based expression vectors have been described for PTP α and inactive PTP α ,^[31] SHP2 and mutants,^[27a] and all other purified PTPs.^[15] PTP activity of the recombinant PTPs was determined in solution, using *para*-nitrophenylphosphate (pNPP) as substrate. The reaction was conducted in a mixture (200 μL) containing 20 mM 2-(*N*-morpholino)ethanesulfonic acid (MES) pH 6.0, 150 mM NaCl, 1 mM ethylenediaminetetraacetic acid (EDTA), 1 mM DTT, and 10 mM pNPP. The reaction was initiated by the addition of fusion protein and incubated at 30 °C. 1 M NaOH (1 mL) was added to quench the reaction and the formation of *p*-nitrophenol was detected with a spectrophotometer at 405 nm.

General procedure for recombinant PTP microarray experiments and profiling

A suitable buffer, for example, a Tris (25 μL , 20 mM, pH 7.4, modified with 50 mM NaCl, 5 mM EDTA, and 1 mM DTT) or a phosphate buffer (25 μL , 25 mM, pH 7.4, modified with 50 mM NaCl, 5 mM EDTA and 1 mM DTT), was used to dissolve the appropriate phosphatase (0.5 mU) together with bovine serum albumin (BSA; 0.25 μL , 10 mg mL⁻¹, Sigma-Aldrich), anti-nitrotyrosine (mouse) an-

tibody (0.5 μL , 0.5 mg mL⁻¹ in PBS pH 7.4, Invitrogen), FITC-goat anti-mouse antibody (0.5 μL , 4 $\mu\text{g mL}^{-1}$, Santa Cruz Biotechnology), and either additional factors, such as an *ortho*-vanadate (Sigma-Aldrich) solution, or water. The resulting mixture was added to PamChip microarrays and the fluorescence was imaged in real time using a Pamstation 12 instrument. The images were analyzed using the Bionavigator software package (PamGene International Ltd.). After automated gridding of the spots, the total fluorescence intensity of each spot was corrected for background fluorescence and the resulting corrected intensity versus cycle progress curves were fitted to the Michaelis–Menten time-course rate equation. The v_{ini} values were then calculated as the reaction speed at $t=5$ cycles. For the calculation of the K_{m} values, the resulting v_{ini} values were plotted against spot concentration and fitted with a global fitting algorithm using the Michaelis–Menten equation.

Vanadate inhibition experiments

Similar conditions as those described above for the recombinant assay were employed, however, part of the water was replaced by solutions of sodium *ortho*-vanadate in water. These inhibitor solutions were serial dilutions from a 1 M stock solution that was heated to 95 °C for 10 min prior to use. Data analysis was carried out as described above for the recombinant PTPs. The resulting v_{ini} values were plotted against spot concentration and fitted using a global fitting algorithm with the equation for competitive inhibition.

Comparison of PY20 and HM11 detection

This assay was either carried out using the conditions for the recombinant PTPs as described above, or under similar conditions in which the two antibodies were replaced by a 1 mg mL⁻¹ solution of the PY20 antibody (0.25 μL , Exalpa Biologicals) and water (0.75 μL). The time-course profiles were determined by gridding and spot analysis as described above for the recombinant PTPs. The rate constants were calculated by fitting to the Michaelis–Menten time course equation.

EnzChek phosphate production assay

The EnzChek phosphate assay kit (Invitrogen) was used using a slightly modified procedure in a miniaturized 96-well format. A 1 mM stock solution of 2-amino-6-mercapto-7-methylpurine riboside (MESG) was prepared in water, as well as a 100 U mL⁻¹ stock solution of purine nucleoside phosphatase in water. To each well a mixture of purified recombinant PTP1B (1 μL corresponding to 0.5 mU), the Tris-based 20 \times strength reaction buffer provided with the kit (5 μL), MESG stock solution (20 μL), purine nucleoside phosphatase stock solution (1 μL), a 40 mM solution of DTT in water (3 μL), and water (20 μL) was added. Then serial dilutions of a 2 mM stock solution of the STAT3 substrate peptide of interest were added (50 μL). The absorption at 360 nm was monitored kinetically in a Biotek μ Quant spectrophotometer. From the linear part of the curve v_{ini} values were calculated after calibration with absorption data obtained with a concentration series of inorganic phosphate. These were corrected with a negative control in which the enzyme solution was replaced by water. The K_{m} value was calculated using a global fitting algorithm with the Michaelis–Menten equation.

Inhibition assay with SHP2 and NSC87877

Similar conditions as described above for the recombinant PTPs were used with the SHP2 enzyme. Part of the water in the mixture was replaced by serial dilutions of a 100 μM stock solution of NSC87877 in water (2.5 μL). Data acquisition and analysis was carried out as described above for the vanadate inhibition experiments.

Preparation of lysates

HEK293 cells were grown in Dulbecco's modified Eagle's medium (DMEM) supplemented with 7.5% fetal calf serum (FCS). HEK293 cells were transiently transfected using polyethylenimine (PEI) with the previously described^[30b] CMV-promoter-driven expression vector for PTP1B, catalytically inactive C215S PTP1B, or empty vector (pCS2+) as a control. After transfection the cells were grown for 40 h in a serum-containing medium before harvesting. The cells were lysed for 20 min on ice in cell lysis buffer (50 mM HEPES pH 7.4, 150 mM NaCl, 1 mM ethylene glycol tetraacetic acid (EGTA), 1.5 mM MgCl_2 , 1% Triton X-100, 10% glycerol, 5 mM NaF, 5 mM β -glycerophosphate, 1 $\mu\text{g mL}^{-1}$ leupeptin, and 1 $\mu\text{g mL}^{-1}$ aprotinin). The lysates were collected using a rubber policeman and centrifuged for 10 min at 13000 rpm. Protein concentrations in the lysates were determined using the BCA test.

Lysate PTP microarray experiments

Similar conditions as described above for the recombinant assay were employed, however, to reduce aspecific interactions leading to clogging of the microarrays and a decreased signal-to-noise ratio, they were first blocked with 2% BSA (aq) for 15 min. Instead of enzyme in buffer, as in the experiments described above, a suitable volume of lysate (corresponding to 1.0 μg total protein) was used, to which phosphate buffer (2.5 μL) $10\times$ strength was added in combination with the remaining factors as described above in the general procedure for recombinant PTPs. In the case of the spiked lysate, a solution of purified recombinant PTP1B was added equal to 1 mU as judged by the *para*-nitrophenylphosphate test. In the vanadate inhibition experiments, a sufficient amount of a 1 M sodium *ortho*-vanadate solution that was heated to 95°C for 10 min prior to use was added to reach a final concentration of 250 μM . Finally, sufficient water was added to obtain a final volume of 25 μL . Data analysis was carried out as described above for the recombinant PTPs.

Acknowledgements

The Netherlands Proteomics Centre (NPC) is acknowledged for funding part of the research (J.A.).

Keywords: enzymes · high-throughput screening · kinetics · microarrays · protein modifications

- [1] a) Y. Xu, G. J. Fisher, *J. Cell Commun. Signal.* **2012**, *6*, 125–138; b) P. Cohen, D. R. Alessi, *ACS Chem. Biol.* **2013**, *8*, 96–104; c) J. Zhang, P. L. Yang, N. S. Gray, *Nat. Rev. Cancer* **2009**, *9*, 28–39; d) N. K. Tonks, *FEBS J.* **2013**, *280*, 346–378.
- [2] a) L. M. Scott, H. R. Lawrence, S. M. Sebt, N. J. Lawrence, J. Wu, *Curr. Pharm. Des.* **2010**, *16*, 1843–1862; b) L. Bialy, H. Waldmann, *Angew. Chem.* **2005**, *117*, 3880–3906; *Angew. Chem. Int. Ed.* **2005**, *44*, 3814–3839; c) J. Becker, *Nat. Biotechnol.* **2004**, *22*, 15–18; d) S. G. Julien, N.

- Dubé, S. Hardy, M. L. Tremblay, *Nat. Rev. Cancer* **2011**, *11*, 35–49; e) A. P. Combs, *J. Med. Chem.* **2010**, *53*, 2333–2344.
- [3] C. H. S. Lu, K. Liu, L. P. Tan, S. Q. Yao, *Chem. Eur. J.* **2012**, *18*, 28–39.
- [4] a) L. Gao, H. Sun, S. Q. Yao, *Biopolymers* **2010**, *94*, 810–819; b) M. Köhn, M. Gutierrez, P. Jonkheijm, S. Wetzel, R. Wacker, H. Schroeder, H. Prinz, C. M. Niemeyer, R. Breinbauer, S. E. Szedlacsek, H. Waldmann, *Angew. Chem.* **2007**, *119*, 7844–7847; *Angew. Chem. Int. Ed.* **2007**, *46*, 7700–7703; c) L. Q. Gao, M. Uttamchandani, S. Q. Yao, *Chem. Commun.* **2012**, *48*, 2240–2242; d) H. Sun, C. H. S. Lu, M. Uttamchandani, Y. Xia, Y. Liou, S. Q. Yao, *Angew. Chem.* **2008**, *120*, 175–178; *Angew. Chem. Int. Ed.* **2008**, *47*, 1698–1702; e) M. Garaud, D. Pei, *J. Am. Chem. Soc.* **2007**, *129*, 5366–5367; f) S. Wächtle, X. Espanel, A. Harrenga, M. Rossi, G. Cesareni, R. Hooft van Huijsduijnen, *J. Biol. Chem.* **2004**, *279*, 311–318.
- [5] A. K. Bose, K. A. Janes, *Mol. Cell. Proteomics* **2013**, *12*, 797–806.
- [6] L. Ren, X. Chen, R. Luechapanichkul, N. G. Selner, T. M. Meyer, A.-S. Wavreille, R. Chan, C. Iorio, X. Zhou, B. G. Neel, D. Pei, *Biochemistry* **2011**, *50*, 2339–2356.
- [7] K. A. Kalesh, L. P. Tan, K. Lu, L. Gao, J. Wang, S. Q. Yao, *Chem. Commun.* **2010**, *46*, 589–591.
- [8] R. Wisastra, K. Poelstra, R. Bischoff, H. Maarsingh, H. J. Haisma, F. J. Dekker, *ChemBioChem* **2011**, *12*, 2016–2020.
- [9] J. Yang, Z. Cheng, T. Niu, X. Liang, Z. J. Zhao, G. W. Zhou, *J. Biol. Chem.* **2000**, *275*, 4066–4071.
- [10] a) H. Honda, J. Inazawa, J. Nishida, Y. Yazaki, H. Hirai, *Blood* **1994**, *84*, 4186–4194; b) K. K. Balavenkatraman, E. Jandt, K. Friedrich, T. Kautenburger, B. L. Bool-Zobel, A. Östman, F. D. Böhmer, *Oncogene* **2006**, *25*, 6319–6324; c) P. E. Thomas, B. L. Wharram, M. Goyal, J. E. Wiggins, L. B. Holzman, R. C. Wiggins, *J. Biol. Chem.* **1994**, *269*, 19953–19961; d) T. Motiwala, N. Zanesi, J. Datta, S. Roy, H. Kutay, A. M. Checovich, M. Kaou, Y. M. Zhong, A. J. Johnson, D. M. Lucas, N. A. Heerema, J. Hagan, X. K. Mo, D. Jarjoura, J. C. Byrd, C. M. Croce, S. T. Jacob, *Blood* **2011**, *118*, 6132–6140.
- [11] S. Thareja, S. Aggarwal, T. R. Bhardwaj, M. Kumar, *Med. Red. Rev.* **2012**, *32*, 459–517.
- [12] a) C. C. van Niekerk, L. G. Poels, *Cancer Lett.* **1999**, *137*, 61–73; b) M. della Peruta, G. Martinelli, E. Moratti, D. Pintani, M. Vezzalini, A. Mafficini, T. Grafone, I. Iacobucci, S. Soverini, M. Murineddu, F. Vinante, C. Tecchio, G. Piras, A. Gabbas, M. Monne, C. Sorio, *Cancer Res.* **2010**, *70*, 8896–8906.
- [13] a) B. N. Ames, *Methods Enzymol.* **1966**, *8*, 115–118; b) H. H. Hess, J. E. Derr, *Anal. Biochem.* **1975**, *63*, 607–613; c) M. R. Webb, *Proc. Natl. Acad. Sci. USA* **1992**, *89*, 4884–4887.
- [14] a) R. Hilhorst, L. Houkes, A. van den Berg, R. Ruijtenbeek, *Anal. Biochem.* **2009**, *387*, 150–161; b) A. J. Poot, J. van Ameijde, M. Slijper, A. van den Berg, R. Hilhorst, R. Ruijtenbeek, D. T. S. Rijkers, R. M. J. Liskamp, *ChemBioChem* **2009**, *10*, 2042–2051; c) S. Lemeer, R. Ruijtenbeek, M. W. H. Pinkse, C. Joplring, A. J. R. Heck, J. den Hertog, M. Slijper, *Mol. Cell. Proteomics* **2007**, *6*, 2088–2099; d) N. Parera Pera, H. M. Branderhorst, R. Kooij, C. Maierhofer, M. van der Kaaden, R. M. J. Liskamp, V. Wittman, R. Ruijtenbeek, R. J. Pieters, *ChemBioChem* **2010**, *11*, 1896–1904; e) H. M. Branderhorst, R. Ruijtenbeek, R. M. J. Liskamp, R. J. Pieters, *ChemBioChem* **2008**, *9*, 1836–1844; f) A. Koppen, R. Houtman, D. Pijnenburg, E. H. Jenning, R. Ruijtenbeek, E. Kalkhoven, *Mol. Cell. Proteomics* **2009**, *8*, 2212–2226.
- [15] A. J. Barr, E. Ugochukwu, H. H. Lee, O. N. F. King, P. Filippakopoulos, I. Alfano, P. Savitsky, N. A. Burgess-Brown, S. Müller, S. Knapp, *Cell* **2009**, *136*, 352–363.
- [16] Y. Hatta, N. Tsuchiya, M. Matsushita, M. Shiota, K. Hagiwara, K. Tokunaga, *Immunogenetics* **1999**, *49*, 280–286.
- [17] A. D. Hamblin, T. J. Hamblin, *Expert Opin. Ther. Targets* **2005**, *9*, 1165–1178.
- [18] R. van Beuningen, H. van Damme, P. Boender, N. Bastiaensen, A. Chan, T. Kievits, *Clin. Chem.* **2001**, *47*, 1931.
- [19] a) J. C. A. ter Steege, L. Koster-Kamphuis, E. A. van Straaten, P. P. Forget, W. A. Buurman, *Free Radical Biol. Med.* **1998**, *25*, 953–963; b) I. Girault, A. E. Karu, M. Schaper, M. H. Barcellos-Hoff, T. Hagen, D. S. Vogel, B. N. Ames, S. Christen, M. K. Shigenaga, *Free Radical Biol. Med.* **2001**, *31*, 1375–1387.
- [20] J. S. Beckmann, Y. Z. Ye, P. G. Anderson, J. Chen, M. A. Accavitti, M. M. Tarpey, C. R. White, *Biol. Chem. Hoppe-Seyler* **1994**, *375*, 81–88.

- [21] a) Z. Zhang, D. Maclean, D. J. McNamara, J. E. Dixon, *Biochemistry* **1994**, *33*, 2285–2290; b) Z. Zhang, A. M. Thieme-Sefler, D. Maclean, D. J. McNamara, E. M. Dobrusin, T. K. Sawyer, J. E. Dixon, *Proc. Natl. Acad. Sci. USA* **1993**, *90*, 4446–4450; c) K. L. Hippen, S. Jakes, J. Richards, B. P. Jena, B. L. Beck, L. B. Tabatabai, T. S. Ingebritsen, *Biochemistry* **1993**, *32*, 12405–12412; d) M. Ruzzene, A. Donella-Deana, O. Marin, J. W. Perich, P. Ruzza, G. Borin, A. Calderan, L. A. Pinna, *Eur. J. Biochem.* **1993**, *211*, 289–295.
- [22] a) J. Montalibet, K. Skorey, D. McKay, G. Scapin, E. Asante-Appiah, B. P. Kennedy, *J. Biol. Chem.* **2006**, *281*, 5258–5266; b) P. G. Drake, G. H. Peters, H. S. Andersen, W. Hendriks, N. P. H. Møller, *Biochem. J.* **2003**, *373*, 393–401.
- [23] U. Dechert, M. Adam, K. W. Harder, I. Clark-Lewis, F. Jirik, *J. Biol. Chem.* **1994**, *269*, 5602–5611.
- [24] G. Huyer, S. Liu, J. Kelly, J. Moffat, P. Payette, B. Kennedy, G. Tsaprailis, M. J. Gresser, *J. Biol. Chem.* **1997**, *272*, 843–851.
- [25] L. Chen, S. Sung, M. L. R. Yip, H. R. Lawrence, Y. Ren, W. C. Guida, S. M. Sebt, N. J. Lawrence, J. Wu, *Mol. Pharmacol.* **2006**, *70*, 562–570.
- [26] J.-H. Zhang, T. D. Y. Chung, K. R. Oldenburg, *J. Biomol. Screening* **1999**, *4*, 67–73.
- [27] a) C. Jopling, D. van Geemen, J. den Hertog, *PLoS Genet.* **2007**, *3*, e225; b) C. Persson, T. Sjöblom, A. Groen, K. Kappert, U. Engström, U. Hellman, C. Heldin, J. den Hertog, *Proc. Natl. Acad. Sci. USA* **2004**, *101*, 1886–1891.
- [28] R. M. Krypta, H. Su, L. F. Reichardt, *J. Cell. Biol.* **1996**, *134*, 1519–1529.
- [29] K.-J. Yang, S. Shin, L. Piao, E. Shin, Y. Li, K. A. Park, H. S. Byun, M. Wo, J. Hong, G. R. Kweon, G. M. Hur, J. H. Seok, T. Chun, D. P. Brazil, B. A. Hemmings, J. Park, *J. Biol. Chem.* **2008**, *283*, 1480–1491.
- [30] a) Z. Jia, D. Barford, A. J. Flint, N. K. Tonks, *Science* **1995**, *268*, 1754–1758; b) A. M. van der Sar, J. de Fockert, M. Betist, D. Zivkovic, J. den Hertog, *Int. J. Dev. Biol.* **1999**, *43*, 785–794.
- [31] J. den Hertog, S. Tracy, T. Hunter, *EMBO J.* **1994**, *13*, 3020–3032.

Received: August 20, 2013

Published online on September 17, 2013